Visual Neuroscience

ARTICLE

Open Access

https://doi.org/10.48130/vns-0026-0017

Visual Neuroscience **2026**, 43: e020

Association between photoreceptor patterns and retinal detachment in myopia: a population-based study

Jianqi Chen[1#], Yangyang Li[1#], Yunhong Shi[1#], Zhidong Li[1#], Shengsong Xu[1,2], Yangjiani Li[1], Yehong Zhuo[1*], Yingting Zhu[1*] and Lei Lei[1*]

[1] *State Key Laboratory of Ophthalmology, Zhongshan Ophthalmic Center, Sun Yat-sen University; Guangdong Provincial Key Laboratory of Ophthalmology and Visual Science, Guangzhou 510060, China*

[2] *Shenzhen Eye Hospital, Shenzhen Eye Medical Center, Southern Medical University, Shenzhen 518040, China*

[#] Authors contributed equally: Jianqi Chen, Yangyang Li, Yunhong Shi, Zhidong Li

[*] Correspondence: zhuoyh@mail.sysu.edu.cn (Zhuo Y); zhuyt35@mail.sysu.edu.cn (Zhu Y); leilei25@mail.sysu.edu.cn (Lei L)

Abstract

Myopia is associated with retinal detachment (RD), a sight-threatening condition. This study aimed to determine whether specific myopic photoreceptor (PR) thickness profiles are associated with RD. In total, 10,328 myopic participants from the UK Biobank who underwent baseline optical coherence tomography (OCT) imaging were included. Thickness measurements of the external limiting membrane (ELM) to the inner and outer photoreceptor segments (ISOS) and from the ISOS to the retinal pigment epithelium (RPE) were obtained via OCT to serve as indicators of the inner and outer photoreceptor segments. Latent profile analysis categorized participants into distinct photoreceptor thickness profiles, and Cox's proportional hazard models were used to estimate the hazard ratios (HRs) of RD between the profiles. Two distinct photoreceptor thickness profiles were identified; Profile 2 (including 142 high myopia participants and 862 low/moderate myopia participants) demonstrated thicker ELM–ISOS and thinner ISOS–RPE measurements than Profile 1 (including 612 high myopia participants and 8,712 low/moderate myopia participants). After adjustment for all covariates (including demographic factors [age, gender, and ethnicity], socioeconomic factors [education and Townsend deprivation index], systemic factors [body mass index, high blood pressure, and diabetes], lifestyle factors [physical activity, sleep duration, smoking status, and drinking status], and ocular factors [intraocular pressure and mean spherical equivalent]), Profile 2 was associated with a significantly increased RD risk compared with Profile 1 (HR, 1.79; 95% confidence interval [CI], 1.07–2.99; $p = 0.027$). These findings suggest that photoreceptor thickness patterns may serve as novel indicators for myopic RD risk assessment.

Citation: Chen J, Li Y, Shi Y, Li Z, Xu S, et al. 2026. Association between photoreceptor patterns and retinal detachment in myopia: a population-based study. *Visual Neuroscience* 43: e020 https://doi.org/10.48130/vns-0026-0017

Introduction

It is projected that from 2000 to 2050, the global prevalence of myopia will increase from 22.9% to 49.8%, whereas the prevalence of high myopia is expected to rise from 2.7% to 9.8%[1]. This trend may be attributed to reduced time spent outdoors and an increase in near work activities[2]. Myopia is associated with significant ocular complications, one of the most severe being retinal detachment (RD), a serious and common sight-threatening emergency[3–5]. RD is characterized by the pathological separation of the neurosensory retina from the underlying retinal pigment epithelium (RPE). The annual incidence of RD ranges from 6.3 to 17.9 per 100,000 individuals and a prevalence of approximately 1%[6].

Variations in photoreceptor (PR) thickness could potentially indicate the PRs' structural vulnerability[7,8]. Although RD most commonly originates in the peripheral retina, myopia-related retinal stretching and chorioretinal degeneration are typically diffuse processes affecting both central and peripheral retinal structures. Therefore, alterations in macular PR thickness patterns may reflect generalized retinal structural susceptibility that predisposes myopic eyes to RD. However, the relationship between PR thickness patterns and susceptibility to RD in myopia remains insufficiently investigated, and the specific PR characteristics that warrant closer monitoring or early intervention have yet to be fully elucidated.

In this study, we aimed to investigate whether specific patterns of PR thickness are associated with a higher longitudinal risk of RD in myopia, using data from the UK Biobank. We applied latent profile analysis (LPA), an exploratory, person-centered approach, to identify and classify myopic participants into latent groups according to their PR thickness patterns[9].

Materials and methods

Study sample

The UK Biobank (www.ukbiobank.ac.uk) is a large-scale prospective cohort study. Recruitment was carried out at assessment centers located across England, Scotland, and Wales. The data collection includes a broad range of details covering the participants' demographic backgrounds, daily habits, health conditions, clinical measurements, and biological specimens. This study was conducted using the UK Biobank resource (Application Number 95829), with ethical approval from the North West–Haydock Research Ethics Committee (reference 21/NW/0157), and the study complied with the principles outlined in the Declaration of Helsinki.

Myopia data

In the UK Biobank study, refractive error was assessed utilizing the Tomey RC 5,000 device (Tomey Corp., Nagoya, Japan). Refractometry results deemed to be unreliable, based on error codes recorded, were excluded from the analysis. Furthermore, individuals with a history of ocular surgeries, such as cataract surgery, refractive laser eye surgery, glaucoma or high intraocular pressure surgery or laser

treatment, or corneal graft surgery, were excluded from the analysis. The mean spherical equivalent (MSE) refractive error was calculated using the formula Spherical Power + (0.5 × Cylindrical Power). An MSE of −0.75 D or lower was used to define individuals with myopia for subsequent analysis[10].

Optical coherence tomography data

In the UK Biobank study, a subset of participants underwent retinal optical coherence tomography (OCT) imaging during their initial examinations using the Topcon 3D OCT-1000 Mk2 (Topcon Corp., Tokyo, Japan)[11]. As quality control procedures, we excluded scans with an image quality score (signal strength) below 45[12,13]. Furthermore, we used some quality indicators to identify and exclude scans with insufficient quality, including the inner limiting membrane (ILM) indicator, validity count, minimum motion correlation, maximum motion delta, and maximum motion factor[12,13]. The ILM measure evaluates the strength of the boundary around the ILM across the entire scan, facilitating the detection of issues such as blinks, areas with significant signal loss, and segmentation problems. The validity count identifies scans that exhibit substantial clipping in the *z*-axis dimension of the OCT image. Motion indicators, which analyze both the nerve fiber layer and total retinal thickness, were used calculate Pearson's correlations and absolute differences between thickness measurements from consecutive B-scans. The lowest correlation and the largest absolute difference in each scan were utilized to generate scores that elucidate potential issues such as blinks and eye movements[12,13]. We then applied the segmentation- and motion-related quality control indicators provided by the UK Biobank Eye Vision Consortium, using their recommended cutoffs to filter scans with unreliable boundaries or substantial motion artifacts, including the ILM indicator (threshold: 0), the validity count indicator (threshold: 744), minimum motion correlation (threshold: 0.63), maximum motion delta (threshold: 3.6), and maximum motion factor (threshold: 1.0)[14].

Following the exclusion of participants with inadequate OCT quality, analysis of the PR parameters was conducted, encompassing measurement of the thickness of the external limiting membrane (ELM) to the inner and outer PR segments (ISOS) and from the ISOS to the RPE across the central, inner, and outer subfields[7]. The spatial definitions of the central, inner, and outer subfields followed the Early Treatment Diabetic Retinopathy Study (ETDRS) grid used in the UK Biobank OCT dataset. Specifically, the central subfield spans a 1-mm diameter centered on the fovea, the inner subfield covers the annulus from 1–3 mm, and the outer subfield covers the annulus from 3–6 mm from the foveal center[7]. ELM–ISOS and ISOS–RPE measurements serve as proxies for the inner and outer PR segments, respectively[7,15]. To ensure comparable contributions in latent profile analysis (LPA), all variables were standardized.

Latent profile analysis

LPA was conducted to explore the latent profiles of the PR among individuals with myopia. The LPA model incorporated PR thickness measurements from multiple macular regions simultaneously, including ELM–ISOS and ISOS–RPE thickness in the central, inner, and outer ETDRS subfields. Therefore, the identified profiles represent distinct multivariate patterns of PR thickness across these regions. Four distinct models were used to estimate the profiles. Model A, which assumes equal variances and sets the covariances to zero, is highly restrictive. In this framework, it is presumed that the variances of the variables remain consistent across all profiles, and the interrelationships between the variables are not calculated. This approach simplifies the model by using fewer degrees of freedom to interpret the data. Model B, on the other hand, allows for varying variances while keeping the covariances at zero, offering more flexibility than Model A by permitting different variances across profiles. Model C, which assumes both equal variances and covariances, integrates additional information that could improve the understanding of the profiles and potentially provide a more detailed explanation of the data. Lastly, Model D, characterized by both varying variances and covariances, is the most intricate, allowing for a more comprehensive examination of the relationships among the variables that define the profiles[16].

To evaluate the optimal number of profiles (the maximum was set to five to ensure a sufficient sample size in each profile) and the optimal model, we compared the Akaike information criterion (AIC) and Bayesian information criterion (BIC), with lower values indicating superior fit. The AIC was calculated as −2 times the log-likelihood and adjusted for the number of parameters, whereas the BIC was also derived as −2 times the log-likelihood but included a penalty based on the number of parameters relative to the sample size[17]. Entropy was used as an indicator of classification accuracy, and an entropy value > 0.80 was considered to be acceptable for reliable profile assignment[18]. Therefore, model selection was restricted to solutions with adequate entropy. Among these eligible models, the final model was determined primarily by the AIC and BIC.

Definition and ascertainment of RD incidence

With reference to a previous study investigating myopia and RD in the UK Biobank[5], the following criteria were used to identify cases of RD: International Classification of Diseases (10th edition) (ICD-10) diagnosis codes H33 and ICD-9 diagnosis codes 361. Participants with RD at baseline were excluded. The follow-up period lasted from the time the participants completed the baseline assessment until the first occurrence of RD, death, or censoring.

Covariates

The following covariates were considered when investigating the association between myopic PR thickness profiles and RD, including demographic factors (age, gender, and ethnicity), socioeconomic factors (education, Townsend deprivation index [TDI]), systemic factors (body mass index [BMI], classified into four categories: Underweight, normal weight, overweight, and obese[19]; high blood pressure [HBP]; diabetes), lifestyle factors (ideal physical activity [yes or no], sleep duration, smoking status [never, former, or current], drinking status [never, former, or current]), and ocular factors (intraocular pressure [IOP] and MSE).

The TDI is a well-established measure of socioeconomic status in UK populations, wherein higher scores indicate lower socioeconomic standing[20]. Physical activity was measured utilizing the International Physical Activity Questionnaire, with ideal activity defined as achieving either 150 min of moderate-intensity exercise, 75 min of vigorous-intensity exercise, or a combination totaling 150 min per week[21]. The corneal-compensated IOP was also incorporated as a covariate, assessed by an Ocular Response Analyzer (Reichert, Buffalo, New York, USA)[22].

Statistical analysis

Following the selection of the optimal model and profiles, we analyzed the distribution of PR thickness and covariates by profiles. Normally distributed variables, as assessed by the Kolmogorov–Smirnov test, were reported as mean ± standard deviation and

compared using *t*-tests for two profiles and one-way analysis of variance for three or more profiles. Non-normally distributed variables are presented as the median (interquartile range, IQR) and compared using the Wilcoxon rank-sum test for two profiles and the Kruskal–Wallis test for three or more profiles. Categorical variables are expressed as numbers (percentages) and compared using the χ^2 test.

To investigate the association between PR thickness profiles and RD, we used Cox's proportional hazard regression models. Three models were constructed: Model 1 was unadjusted; Model 2 was adjusted for age, gender, and ethnicity; and Model 3 included further adjustments for all covariables, including age, gender, ethnicity, education, TDI, BMI, HBP, diabetes, physical activity, sleep duration, smoking status, drinking status, IOP, and MSE. Multicollinearity in Model 3 was assessed using generalized variance inflation factors (GVIFs). For variables with more than one degree of freedom, we reported $GVIF^{1/(2 \times Df)}$ as a standardized measure that was comparable across predictors.

We further conducted subgroup analyses based on age (middle-aged adults/older adults, categorized using a threshold of 60 years old)[23], gender (male/female), ethnicity (White/non-White), ideal physical activity (yes/no), sleep duration (short/long, categorized using the median levels of the participants), IOP (low/high, categorized using the median levels of the participants), and MSE (low/high, categorized using the median levels of the participants). Interaction effects were evaluated by incorporating interaction terms between PR thickness profiles and stratified variables. The *p*-value < 0.05 for the interaction was considered to be a statistically significant interaction effect.

Data analyses were performed using R 4.4.0 (R Foundation, Vienna, Austria). All tests of significance were two-sided, and *p*-values < 0.05 were considered to be statistically significant.

Results

Latent profile of PR thickness

Among the various models and classification strategies, 10 demonstrated satisfactory classification performance (entropy values > 0.8). Among these, Model D with two profiles was deemed to be the most appropriate option because it had the lowest BIC and AIC values (Table 1).

Two latent profiles of PR thickness were subsequently identified among individuals with myopia. Compared with profile 1 paticipants (N = 9,324), Profile 2 participants (N = 1,004) exhibited relatively thicker ELM–ISOS thicknesses in the central (Z-score: 0.33, IQR, −0.44 to 1.90), inner (Z-score: 1.13, IQR, 0.12–2.27), and outer (Z-score: 1.89, IQR, 0.88–2.72) subfields, as well as thinner ISOS–RPE thicknesses in the central (Z-score: −0.51, IQR, −2.38 to 0.37), inner (Z-score: −0.53, IQR, −1.99 to 0.28), and outer (Z-score: −1.15, IQR, −2.48 to 0) subfields (all $p < 0.001$ between the two profiles according to the Wilcoxon rank-sum test) (Fig. 1).

Baseline characteristics

Of the 10,328 participants included, 9,324 were in the Profile 1 group, and 1,004 were in the Profile 2 group. In comparison with those in the Profile 1 group, participants in the Profile 2 group were significantly older (Profile 1: 55.00, IQR: 48.00–61.00; Profile 2: 56.00, IQR, 49.00–62.00; $p < 0.001$) and more likely to be male (54.18% vs. 46.21%, $p < 0.001$). Additionally, they exhibited a higher prevalence of HBP (26.89% vs. 23.96%, $p = 0.043$) and demonstrated a lower MSE (Profile 1: −2.18, IQR: −3.72 to −1.29; Profile 2: −2.85, IQR, −4.87 to −1.72; $p < 0.001$). Profile 1 and Profile 2 participants displayed comparable patterns for ethnicity, education, TDI, BMI, physical activity, sleep duration, smoking and drinking behavior, diabetes, and IOP (Table 2).

PR thickness patterns and RD

Compared with Profile 1 participants, participants in Profile 2 exhibited a significantly increased risk of RD. In Model 1 (unadjusted), the hazard ratio (HR) was 2.23 (95% confidence interval [CI], 1.35–3.68, $p = 0.002$). After adjusting for demographic factors (Model 2), the HR decreased to 2.12 (95% CI, 1.28–3.50, $p = 0.003$). Subsequent full adjustments in Model 3 yielded similar results, with an HR of 1.79 (95% CI, 1.07–2.99, $p = 0.027$), demonstrating a 79% increased risk of RD in Profile 2 PR thickness (Table 3). All $GVIF^{1/(2 \times Df)}$ values were close to 1 (range: 1.004–1.072), indicating negligible multicollinearity.

In subgroup analysis according to age, gender, ethnicity, physical activity, sleep duration, IOP, and MSE, significant associations after full adjustment in Model 3 were documented in individuals who were middle-aged (HR, 2.10, 95% CI, 1.08–4.06, $p = 0.028$), male (HR, 2.24, 95% CI, 1.22–4.10, $p = 0.009$), White (HR, 1.88, 95% CI, 1.10–3.20, $p = 0.021$), had ideal physical activity (HR, 2.65, 95% CI,

Table 1. Model fit indices for the LPA of PR thickness.

Model	Profile	AIC	BIC	Entropy	Sample proportion (smallest class)	Sample proportion (largest class)
A	2	156,930.18	157,067.79	1.00	0.02	0.98
A	3	147,606.78	147,795.09	0.86	0.02	0.56
A	4	143,841.44	144,080.44	0.83	0.02	0.47
A	5	141,507.19	141,796.89	0.84	0.02	0.44
B	2	151,501.49	151,682.55	0.95	0.07	0.93
B	3	138,565.49	138,840.71	0.88	0.07	0.47
B	4	132,870.19	133,239.56	0.86	0.06	0.39
B	5	130,586.77	131,050.29	0.83	0.06	0.30
C	2	122,149.30	122,395.55	1.00	0.03	0.97
C	3	123,259.51	123,556.46	0.41	0.04	0.53
C	4	119,228.96	119,576.61	0.52	0.00	0.95
C	5	117,364.12	117,762.47	0.62	0.02	0.81
D	2	112,026.30	112,424.64	0.91	0.10	0.90
D	3	109,411.13	110,012.27	0.74	0.09	0.69
D	4	107,692.97	108,496.90	0.75	0.07	0.69
D	5	106,719.06	107,725.78	0.74	0.06	0.53

AIC, Aikake information criterion; BIC, Bayesian information criterion.

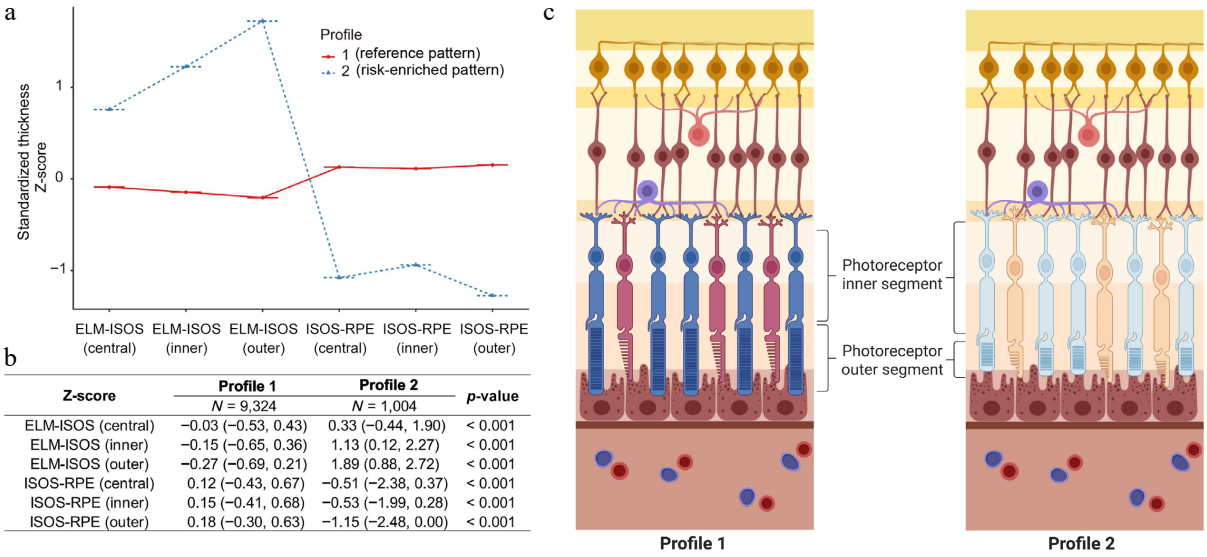

b

Z-score	Profile 1 N = 9,324	Profile 2 N = 1,004	p-value
ELM-ISOS (central)	−0.03 (−0.53, 0.43)	0.33 (−0.44, 1.90)	< 0.001
ELM-ISOS (inner)	−0.15 (−0.65, 0.36)	1.13 (0.12, 2.27)	< 0.001
ELM-ISOS (outer)	−0.27 (−0.69, 0.21)	1.89 (0.88, 2.72)	< 0.001
ISOS-RPE (central)	0.12 (−0.43, 0.67)	−0.51 (−2.38, 0.37)	< 0.001
ISOS-RPE (inner)	0.15 (−0.41, 0.68)	−0.53 (−1.99, 0.28)	< 0.001
ISOS-RPE (outer)	0.18 (−0.30, 0.63)	−1.15 (−2.48, 0.00)	< 0.001

Fig. 1 Distribution of Z-scores for PR thickness, comparing distinct profiles derived via LPA. (a) Distribution of Z-scores among participants. Positive values indicate thicker values relative to the cohort mean; negative values indicate thinner values. (b) Comparison of PR thickness parameters across identified profiles. (c) Visualization of the two identified PR profiles to conceptually summarize the relative differences in the inner and outer PR segments (schematic illustration, not to scale). ELM, external limiting membrane; ISOS, inner and outer PR segments; RPE, retinal pigment epithelium.

1.47–4.78, p = 0.001), had long sleep duration (HR, 2.50, 95% CI, 1.11–5.64, p = 0.027), had low IOP (HR, 2.66, 95% CI, 1.33–5.35, p = 0.006), and had low MSE (HR, 1.84, 95% CI, 1.01–3.35, p = 0.045). However, it is important to note that these associations were observed without significant interaction effects (p for interaction > 0.05), suggesting that the association between PR profiles and RD in myopia was robust across subgroups (Table 3).

Discussion

This study utilized a cohort of 10,328 participants from the UK Biobank to investigate the association between the PR thickness profiles in individuals with myopia and the risk of developing RD. The investigation revealed several key findings. (1) According to the LPA, the myopic PR thickness can be classified into two distinct profiles. (2) Compared with Profile 1, Profile 2 participants exhibited a thicker inner PR segment thickness and a thinner outer PR segment thickness. (3) Myopic participants with Profile 2 PR thickness exhibited an 79% increased risk of RD.

The ISOS–RPE measurement serves as an indirect indicator of the PR's outer segment (POS). The POS comprises multiple layers of plasma membrane discs that contain visual pigments. In healthy retina, the PR maintains a generally stable length by continuously forming new outer segments from the base while also shedding mature outer segments, which are subsequently engulfed by the RPE through phagocytosis[24]. The POS interdigitates with the RPE and is crucial in homeostatic maintenance of the outer retina[25]. Pathological conditions can reduce the POS's length, and thinning of the POS may compromise this interaction, predisposing the retina to detachment under the pathological stress of myopic elongation[26]. The reduction in POS in myopic individuals may also indicate early PR degeneration.

Similarly, the ELM–ISOS measurement is widely considered to be a proxy indicator for the PR's inner segment (PIS)[7]. In this study, we observed that the PR thickness profiles with a higher RD risk exhibited a thicker ELM–ISOS measurement. As mitochondria are prominent in the inner segments, abnormalities in the outer retina can induce mitochondrial swelling, leading to a thickening in the PIS[27]. According to previous investigations, exposure to particulat matter (PM2.5) and NO_2 exposure were associated with thicker PIS in the UK Biobank data[8]. The pattern we observed may also indicate that patterns with a thicker ELM–ISOS are related to pathological myopic retinal changes.

This study significantly advanced our understanding of the latent group structures of PR thickness in myopia and its associated RD risk. The OCT-derived measurements of PR thickness not only provide insights into the histological patterns in myopic eyes but also serve as potential biomarkers for assessing RD risk. The study exhibits several notable strengths that enhance its validity. First, it used LPA, which offers a person-centered, data-driven approach to discover hidden heterogeneity by objectively identifying and classifying latent subgroups on the basis of multiple variables, enabling more nuanced insights into complex multivariate relationships without a priori assumptions about the group structure. Secondly, it utilizes data from the UK Biobank, a large-scale, ongoing cohort study. By using a longitudinal cohort design, the study effectively examines different PR thickness profiles and their potential association with RD, offering valuable insights into identifying the specific PR thickness profile with an increased RD risk that requires focused attention.

However, the study has some limitations. First, despite highly myopic eyes being at greater risk for RD, we had to expand our research focus to include all myopic individuals because of the relatively limited sample size of high-myopia cases in the UK Biobank. Although this approach provides more generalizable insights across the spectrum of myopia severity, it may dilute the specific patterns that might be more pronounced in highly myopic eyes. Second, our analysis lacked important covariates available, such as a family history of RD, as well as axial length measurements, with MSE being used as a proxy covariate, considering the strong correlation between MSE and axial length[28]. However, this may not fully account for the anatomical elongation characteristics of myopic eyes. Residual confounding from unmeasured axial length cannot be entirely excluded. If axial length is independently associated with both PR thickness patterns and RD risk, incomplete adjustment

Table 2. Baseline characteristics of the participants between PR thickness profiles.

Characteristics	Profile 1 (*N* = 9,324)	Profile 2 (*N* = 1,004)	*p*-Value
Age	55.00 (48.00, 61.00)	56.00 (49.00, 62.00)	< 0.001
Gender			< 0.001
Female	5,015.00 (53.79%)	460.00 (45.82%)	
Male	4,309.00 (46.21%)	544.00 (54.18%)	
Ethnicity			0.193
Non-White	783.00 (8.40%)	97.00 (9.66%)	
White	8,541.00 (91.60%)	907.00 (90.34%)	
Education			0.064
College	4,593.00 (49.26%)	526.00 (52.39%)	
Other levels	4,731.00 (50.74%)	478.00 (47.61%)	
TDI	−1.62 (−3.37, 0.87)	−1.44 (−3.26, 1.26)	0.090
BMI			0.451
Underweight	46.00 (0.49%)	7.00 (0.70%)	
Normal	3,335.00 (35.77%)	338.00 (33.67%)	
Overweight	3,910.00 (41.93%)	427.00 (42.53%)	
Obese	2,033.00 (21.80%)	232.00 (23.11%)	
Ideal physical activity			0.146
No	3,758.00 (40.30%)	429.00 (42.73%)	
Yes	5,566.00 (59.70%)	575.00 (57.27%)	
Sleep duration	7.00 (6.00, 8.00)	7.00 (6.00, 8.00)	0.995
Smoking status			0.495
Never	5,017.00 (53.81%)	556.00 (55.38%)	
Previous	3,258.00 (34.94%)	332.00 (33.07%)	
Current	1,049.00 (11.25%)	116.00 (11.55%)	
Drinking status			0.376
Never	364.00 (3.90%)	43.00 (4.28%)	
Previous	336.00 (3.60%)	44.00 (4.38%)	
Current	8,624.00 (92.49%)	917.00 (91.33%)	
HBP			0.043
No	7,090.00 (76.04%)	734.00 (73.11%)	
Yes	2,234.00 (23.96%)	270.00 (26.89%)	
Diabetes			0.405
No	8,874.00 (95.17%)	949.00 (94.52%)	
Yes	450.00 (4.83%)	55.00 (5.48%)	
IOP	15.80 (13.80, 18.02)	15.96 (13.71, 18.18)	0.320
MSE	−2.18 (−3.72, −1.29)	−2.85 (−4.87, −1.72)	< 0.001

BMI, body mass index; TDI, Townsend deprivation index; HBP, high blood pressure; IOP, intraocular pressure; MSE, mean spherical equivalent. Non-normally distributed variables are presented as median (interquartile range, IQR) and compared using the Wilcoxon rank-sum test. Categorical variables are expressed as numbers (percentages) and compared using the χ^2 test.

could partially influence the estimated HRs. Nevertheless, we incorporated MSE as a covariate in fully adjusted models and additionally conducted subgroup analyses stratified by MSE level. The association between PR profiles and RD remained directionally consistent across MSE strata, suggesting that the observed relationship is unlikely to be solely explained by refractive severity. Future studies incorporating direct axial length measurements are warranted. Third, the UK Biobank PR measurements only provided data on concentric subfields (central, inner, and outer), without directional differentiation of the superior, inferior, nasal, or temporal regions. Future studies incorporating direction-specific measurements would provide more comprehensive insights into the spatial heterogeneity of retinal patterns associated with RD in myopia. Fourth, the subgroup analyses should be interpreted cautiously. Although no statistically significant interaction effects were observed, interaction tests typically require larger sample sizes than main effect analyses to detect effect modification. Given the relatively low incidence of RD and smaller sample sizes in certain subgroups (e.g., non-White participants), our study may have been underpowered to detect modest interaction effects. Therefore, the absence of a significant interaction does not definitively exclude potential heterogeneity across subgroups, and future studies with larger event numbers are warranted. Fifth, as UK Biobank is a population-based cohort designed for large-scale standardized assessment rather than disease-specific deep phenotyping, highly specialized ophthalmic imaging modalities (e.g., advanced RPE morphometry) were not available. Future dedicated myopia or RD cohorts incorporating multimodal imaging and molecular profiling may further elucidate the mechanistic basis of the identified structural pattern. Another limitation is that RD diagnoses in the UK Biobank are recorded using ICD codes at the participant level rather than the eye level. Consequently, the association between photoreceptor PR patterns and RD risk was evaluated at the participant level. This limitation may introduce some degree of exposure misclassification, although similar approaches have been used in previous UK Biobank-based ophthalmic studies[5]. In addition, different subtypes of retinal detachment may involve distinct pathophysiological mechanisms and could potentially show different relationships with the PRs' structural patterns. However, the number of incident RD cases in this longitudinal cohort was relatively limited, and further stratification

Table 3. Associations between PR thickness profiles and the incidence of RD among individuals with myopia.

		Model 1			Model 2			Model 3		
		HR (95% CI)	*p*-Value	*p*-Value for interaction	HR (95% CI)	*p*-Value	*p*-Value for interaction	HR (95% CI)	*p*-Value	*p*-Value for interaction
Overall		2.23 (1.35–3.68)	0.002	–	2.12 (1.28–3.50)	0.003	–	1.79 (1.07–2.99)	0.027	–
Subgroup analysis										
Age group	Middle-aged adults	2.30 (1.20–4.43)	0.012	0.818	2.23 (1.16–4.29)	0.017	0.807	2.10 (1.08–4.06)	0.028	0.712
	Older adults	2.05 (0.94–4.47)	0.070		1.99 (0.91–4.34)	0.083		1.89 (0.86–4.15)	0.114	
Gender	Female	1.57 (0.61–4.00)	0.347	0.404	1.55 (0.61–3.96)	0.360	0.405	1.34 (0.51–3.51)	0.550	0.388
	Male	2.50 (1.37–4.55)	0.003		2.47 (1.35–4.50)	0.003		2.24 (1.22–4.10)	0.009	
Ethnicity	Non-White	3.24 (0.63–16.72)	0.160	0.641	2.88 (0.56–14.94)	0.208	0.639	2.04 (0.37–11.29)	0.412	0.598
	White	2.16 (1.28–3.66)	0.004		2.06 (1.21–3.49)	0.007		1.88 (1.10–3.20)	0.021	
Ideal physical activity	No	1.06 (0.37–2.98)	0.916	0.073	1.00 (0.35–2.83)	0.999	0.075	0.96 (0.34–2.73)	0.939	0.070
	Yes	3.15 (1.76–5.64)	< 0.001		3.00 (1.68–5.39)	< 0.001		2.65 (1.47–4.78)	0.001	
Sleep duration	Long	2.98 (1.34–6.60)	0.007	0.377	2.69 (1.21–5.99)	0.015	0.392	2.50 (1.11–5.64)	0.027	0.370
	Short	1.88 (0.99–3.60)	0.055		1.84 (0.96–3.51)	0.067		1.68 (0.87–3.23)	0.120	
IOP	High	1.54 (0.73–3.27)	0.255	0.150	1.44 (0.68–3.06)	0.340	0.141	1.36 (0.64–2.89)	0.426	0.190
	Low	3.24 (1.64–6.41)	0.001		3.19 (1.61–6.31)	0.001		2.66 (1.33–5.35)	0.006	
MSE	High	2.16 (0.84–5.58)	0.112	0.918	2.13 (0.82–5.51)	0.120	0.894	2.04 (0.79–5.31)	0.142	0.822
	Low	2.04 (1.13–3.68)	0.018		1.88 (1.04–3.40)	0.038		1.84 (1.01–3.35)	0.045	

HR, hazard ratio; CI, confidence interval; IOP, intraocular pressure; MSE, mean spherical equivalent. Profile 1 PR thickness was set as the reference. In the subgroup analysis, sleep duration, IOP, and MSE were reorganized as binary variables based on the median levels of the participants.

by subtype resulted in insufficient statistical power for a stable estimation. Therefore, RD was analyzed as a single outcome in the present study. Future studies with larger numbers of RD events may allow a more detailed exploration of subtype-specific associations. Moreover, the findings are derived from a UK Biobank cohort, which is known to have a "healthy volunteer" selection bias[29].

Conclusions

In conclusion, this study utilized LPA to elucidate the complex structural variations in PR thickness among myopic individuals and to investigate their association with RD incidence. We identified that a specific retinal pattern characterized by increased inner PR segment thickness and decreased outer PR segment thickness was associated with an elevated risk of RD. These findings not only provide novel insights into the latent group structure of PR in the myopic retina but also offer potential indicators for RD risk. Replication in other large-scale, prospective cohorts will be important to further establish the robustness and clinical applicability of these findings.

Ethical statements

The study was conducted in accordance with the Declaration of Helsinki, and the protocol was approved by the North West Multi-Center Research Ethics Committee (reference 21/NW/0157; dated June 29, 2021). Informed consent for participation was obtained from all subjects involved in the study.

Author contributions

The authors confirm their contributions to the paper as follows: study conception and design: Zhuo Y, Zhu Y, Lei L; data collection: Zhuo Y, Chen J; analysis and interpretation of results: Chen J, Li Y, Shi Y, Li Z; draft manuscript preparation: Chen J, Li Y, Shi Y, Li Z, Xu S, Li Y, Zhu Y. All authors reviewed the results and approved the final version of the manuscript.

Data availability

The data that support the findings of this study are available from the UK Biobank (www.ukbiobank.ac.uk).

Acknowledgments

This study was supported by the National Natural Science Foundation of China (grant numbers 8217040283, 82471074, and 82171057), the Guangdong Basic and Applied Basic Research Foundation (grant number 2024A1515013058), the Science and Technology Program of Guangzhou, China (grant number 202206080005), and the Major Science and Technology Project of Zhongshan City (grant number 2022A1007). This research has been conducted using the UK Biobank data (application number 95829).

Conflict of interest

The authors declare that they have no conflict of interest.

Dates

Received 13 January 2026; Revised 6 March 2026; Accepted 10 March 2026; Published online 1 May 2026

References

[1] Holden BA, Fricke TR, Wilson DA, Jong M, Naidoo KS, et al. 2016. Global prevalence of myopia and high myopia and temporal trends from 2000 through 2050. *Ophthalmology* 123:1036–1042

[2] Jones LA, Sinnott LT, Mutti DO, Mitchell GL, Moeschberger ML, et al. 2007. Parental history of myopia, sports and outdoor activities, and future myopia. *Investigative Opthalmology & Visual Science* 48:3524–3532

[3] Verkicharla PK, Ohno-Matsui K, Saw SM. 2015. Current and predicted demographics of high myopia and an update of its associated pathological changes. *Ophthalmic and Physiological Optics* 35:465–475

[4] van Leeuwen R, Haarman AEG, van de Put MAJ, Klaver CCW, Los LI. 2021. Association of rhegmatogenous retinal detachment incidence with myopia prevalence in the Netherlands. *JAMA Ophthalmology* 139:85–92

[5] Han X, Ong JS, An J, Craig JE, Gharahkhani P, et al. 2020. Association of myopia and intraocular pressure with retinal detachment in European descent participants of the UK Biobank cohort: a mendelian randomization study. *JAMA Ophthalmology* 138:671–678

[6] Mitry D, Charteris DG, Fleck BW, Campbell H, Singh J. 2010. The epidemiology of rhegmatogenous retinal detachment: geographical variation and clinical associations. *British Journal of Ophthalmology* 94:678–684

[7] Chua SYL, Dhillon B, Aslam T, Balaskas K, Yang Q, et al. 2019. Associations with photoreceptor thickness measures in the UK Biobank. *Scientific Reports* 9:19440

[8] Chua SYL, Warwick A, Peto T, Balaskas K, Moore AT, et al. 2022. Association of ambient air pollution with age-related macular degeneration and retinal thickness in UK Biobank. *British Journal of Ophthalmology* 106:705–711

[9] Berlin KS, Williams NA, Parra GR. 2014. An introduction to latent variable mixture modeling (part 1): overview and cross-sectional latent class and latent profile analyses. *Journal of Pediatric Psychology* 39:174–187

[10] Guggenheim JA, Williams C. 2015. Role of educational exposure in the association between myopia and birth order. *JAMA Ophthalmology* 133:1408–1414

[11] Ko F, Foster PJ, Strouthidis NG, Shweikh Y, Yang Q, et al. 2017. Associations with retinal pigment epithelium thickness measures in a large cohort: results from the UK Biobank. *Ophthalmology* 124:105–117

[12] Madjedi KM, Stuart KV, Chua SYL, Ramulu PY, Warwick A, et al. 2023. The association of physical activity with glaucoma and related traits in the UK Biobank. *Ophthalmology* 130:1024–1036

[13] Chen J, Huang S, Zhuo X, Chen X, Xie R, et al. 2025. Association between outdoor daylight exposure duration and primary open-angle glaucoma. *American Journal of Ophthalmology* 281:162–171

[14] Keane PA, Grossi CM, Foster PJ, Yang Q, Reisman CA, et al. 2016. Optical coherence tomography in the UK Biobank study - rapid automated analysis of retinal thickness for large population-based studies. *PLoS One* 11:e0164095

[15] Spaide RF, Curcio CA. 2011. Anatomical correlates to the bands seen in the outer retina by optical coherence tomography: literature review and model. *Retina* 31:1609–1619

[16] Rosenberg JM, Beymer PN, Anderson DJ, van Lissa CJ, Schmidt JA. 2018. tidyLPA: an R package to easily carry out latent profile analysis (LPA) using open-source or commercial software. *Journal of Open Source Software* 3:978

[17] Wang H, Yang Y, Li G, Wang Y, Wu Y, et al. 2025. Exposure to green space, nighttime light, air pollution, and noise and cardiovascular disease risk: a prospective cohort study. *Environmental Pollution* 367:125603

[18] Lubke G, Muthén BO. 2007. Performance of factor mixture models as a function of model size, covariate effects, and class-specific parameters. *Structural Equation Modeling: A Multidisciplinary Journal* 14:26–47

[19] Luo P, Ying J, Li J, Yang Z, Sun X, et al. 2023. Air pollution and allergic rhinitis: findings from a prospective cohort study. *Environmental Science & Technology* 57:15835–15845

[20] Ye J, Wen Y, Sun X, Chu X, Li P, et al. 2021. Socioeconomic deprivation index is associated with psychiatric disorders: an observational and genome-wide gene-by-environment interaction analysis in the UK Biobank cohort. *Biological Psychiatry* 89:888–895

[21] Lloyd-Jones DM, Hong Y, Labarthe D, Mozaffarian D, Appel LJ, et al. 2010. Defining and setting national goals for cardiovascular health promotion and disease reduction: the American heart association's strategic impact goal through 2020 and beyond. *Circulation* 121:586–613

[22] MacGregor S, Ong JS, An J, Han X, Zhou T, et al. 2018. Genome-wide association study of intraocular pressure uncovers new pathways to glaucoma. *Nature Genetics* 50:1067–1071

[23] Chen J, Cao X, Zhuo X, Chen X, Ling Y, et al. 2025. Relationships between frailty and the risk of glaucoma in middle-aged and older adults. *Ophthalmology Glaucoma* 8:73–82

[24] Kaye RA, Patasova K, Patel PJ, Hysi P, Lotery AJ. 2021. Macular thickness varies with age-related macular degeneration genetic risk variants in the UK Biobank cohort. *Scientific Reports* 11:23255

[25] Boulton M, Dayhaw-Barker P. 2001. The role of the retinal pigment epithelium: topographical variation and ageing changes. *Eye* 15:384–389

[26] Kamoshita M, Ozawa Y, Kubota S, Miyake S, Tsuda C, et al. 2014. AMPK-NF-κB axis in the photoreceptor disorder during retinal inflammation. *PLoS One* 9:e103013

[27] Wilson JD, Bigelow CE, Calkins DJ, Foster TH. 2005. Light scattering from intact cells reports oxidative-stress-induced mitochondrial swelling. *Biophysical Journal* 88:2929–2938

[28] Chen S, Liu X, Sha X, Yang X, Yu X. 2021. Relationship between axial length and spherical equivalent refraction in Chinese children. *Advances in Ophthalmology Practice and Research* 1:100010

[29] Fry A, Littlejohns TJ, Sudlow C, Doherty N, Adamska L, et al. 2017. Comparison of sociodemographic and gealth-related characteristics of UK Biobank participants with those of the general population. *American Journal of Epidemiology* 186:1026–1034